The Astrophysical Journal, 830:131 (9pp), 2016 October 20 doi:10.3847/0004-637X/830/2/131

EVOLUTION OF INTERMEDIATE-MASS X-RAY BINARIES DRIVEN BY THE MAGNETIC BRAKING OF AP/BP STARS. I. ULTRACOMPACT X-RAY BINARIES

Wen-Cong Chen[1,2] and Philipp Podsiadlowski[2]
[1] School of Physics and Electrical Information, Shangqiu Normal University, Shangqiu 476000, China; chenwc@pku.edu.cn
[2] Department of Physics, University of Oxford, Oxford OX1 3RH, UK
Received 2016 June 20; revised 2016 August 5; accepted 2016 August 8; published 2016 October 18

ABSTRACT

It is generally believed that ultracompact X-ray binaries (UCXBs) evolved from binaries consisting of a neutron star accreting from a low-mass white dwarf (WD) or helium star where mass transfer is driven by gravitational radiation. However, the standard WD evolutionary channel cannot produce the relatively long-period (40–60 minutes) UCXBs with a high time-averaged mass-transfer rate. In this work, we explore an alternative evolutionary route toward UCXBs, where the companions evolve from intermediate-mass Ap/Bp stars with an anomalously strong magnetic field (100–10,000 G). Including the magnetic braking caused by the coupling between the magnetic field and an irradiation-driven wind induced by the X-ray flux from the accreting component, we show that intermediate-mass X-ray binaries (IMXBs) can evolve into UCXBs. Using the *MESA* code, we have calculated evolutionary sequences for a large number of IMXBs. The simulated results indicate that, for a small wind-driving efficiency $f = 10^{-5}$, the anomalous magnetic braking can drive IMXBs to an ultra-short period of 11 minutes. Comparing our simulated results with the observed parameters of 15 identified UCXBs, the anomalous magnetic braking evolutionary channel can account for the formation of seven and eight sources with $f = 10^{-3}$, and 10^{-5}, respectively. In particular, a relatively large value of f can fit three of the long-period, persistent sources with a high mass-transfer rate. Though the proportion of Ap/Bp stars in intermediate-mass stars is only 5%, the lifetime of the UCXB phase is $\gtrsim$2 Gyr, producing a relatively high number of observable systems, making this an alternative evolutionary channel for the formation of UCXBs.

Key words: binaries: general – stars: evolution – stars: mass-loss – X-rays: binaries

1. INTRODUCTION

Ultracompact X-ray binaries (UCXBs) are a sub-population of low-mass X-ray binaries (LMXBs) with ultra-short orbital periods (usually less than 1 hr). They are thought to be accretion-powered X-ray sources, in which a neutron star (NS) or a black hole (BH, though BH accretors have not yet been detected in UCXBs) accretes matter from a donor star by Roche-lobe overflow (Savonije et al. 1986). From the orbits of the UCXBs, their donor stars can be constrained to be partially or fully degenerate stars such as white dwarfs (WDs) or helium (He) stars (Rappaport et al. 1982; Nelson et al. 1986; Podsiadlowski et al. 2002; Deloye & Bildsten 2003). In some UCXBs or UCXB candidates, the spectra imply that the transferred material is either mainly composed of He or carbon and oxygen, which provides support for the donor identifications (Nelemans et al. 2004, 2006). So far, there are 15 identified UCXBs, 10 persistent sources, and 5 transient sources.

It is worth pointing out the broad astrophysical significance of UCXBs. They offer important information on stellar and binary evolution, constraining the accretion process, angular-momentum loss mechanisms, and the common-envelope (CE) phase. In addition, UCXBs are thought to be possible gravitational-wave sources, which can be detected by LISA (Nelemans 2009).

In globular clusters, it is generally accepted that UCXBs originated from dynamic processes such as direct collisions (Verbunt 1987; Rasio & Shapiro 1991; Davies et al. 1992; Ivanova et al. 2005; Lombardi et al. 2006; Ivanova et al. 2010), tidal captures (Bailyn & Grindlay 1987; Podsiadlowski et al. 2002), and exchange interactions (Davies & Hansen 1998; Rasio et al. 2000; Ivanova et al. 2010). In the Galactic field, these dynamical processes can safely be ignored. In the field, the donor stars in the progenitor systems of UCXBs include two cases: main-sequence stars and compact WDs or He stars. In standard low/intermediate-mass X-ray binaries (L/IMXBs) with a main-sequence donor star, magnetic braking can drive the binaries to a relatively short period of 2–3 hr. When the donor star becomes fully convective, magnetic braking ceases and gravitational radiation becomes the dominant angular-momentum loss mechanism, possibly leading to the formation of a UCXB. For a binary system consisting of an NS and a (sub)giant, mass transfer may be dynamically unstable. This leads to a CE phase and ultimately the formation of NS + WD or NS + He star binaries with compact orbits. Gravitational radiation will make the orbits shrink until the WDs or He stars fill their Roche lobes and start to transfer material to the NSs. With the further decay of the orbits, the binaries will now appear to be UCXBs (Tutukov & Yungelson 1993; Iben et al. 1995; Yungelson et al. 2002; Belczynski & Taam 2004; van Haaften et al. 2012a).

At present, there exist some intriguing problems in the formation of UCXBs. First, a very narrow range in initial parameters cannot explain the relatively large number of detected UCXBs (van der Sluys et al. 2005a). Second, the evolution toward UCXBs strongly depends on the efficiency of magnetic braking. It is possible that the standard magnetic-braking model overestimates the angular-momentum loss rate (also see Section 3.2). van der Sluys et al. (2005b) found that it is difficult to form UCXBs within a Hubble time under the modified magnetic-braking law given by Queloz et al. (1998) and Sills et al. (2000). Third, van Haaften et al. (2012b) found that the time-averaged luminosity for UCXBs with periods longer than 50 minutes are significantly higher than the

predictions from the theoretical mass-transfer rate. Recently, Heinke et al. (2013) argued that the higher average mass-transfer rates in three persistent UCXBs with relatively long orbital periods (40–60 minutes) cannot be produced by the standard WD evolutionary scenario.

NS + He star binaries can produce the group of UCXBs with long orbital periods (40–60 minutes) and high mass-transfer rates (Heinke et al. 2013). If one includes the tidal torque between the binary and a hypothetical circumbinary disk, this population of UCXBs can evolve from LMXBs if a relatively high fraction ($\delta \gtrsim 0.008$) of the mass transferred is fed to the circumbinary disk (Ma & Li 2009b). However, it is difficult to reproduce the relatively high birth rates for the above two models because of the short lifetime ($\sim 10^7$ years) in the UCXB stage.

To solve some of these problems, a new evolutionary channel to form UCXBs may be required or a more efficient angular-momentum loss mechanism. In this work, we present an alternative evolutionary channel for UCXBs. In this channel, we assume that some intermediate-mass donor stars have an anomalously strong magnetic field (10–10,000 G) and that the magnetic braking is produced by the coupling between the magnetic field and the irradiation-driven wind and show that this can convert IMXBs into UCXBs.

2. DESCRIPTION OF BINARY EVOLUTION

2.1. The Binary Evolution Code

In this work, we calculate the evolution of IMXBs using version 7624 of the Modules for Experiments in Stellar Astrophysics code (MESA; Paxton et al. 2011, 2013, 2015). In particular, MESAbinary is a MESA module that can evolve a binary system including a normal star and a point-mass companion or another star. We start with binary systems consisting of an intermediate-mass donor star (with a mass of $M_{\rm d} = 1.6$–$5.0\,M_\odot$) and an NS (with a mass of $M_{\rm NS} = 1.4\,M_\odot$) in a circular orbit. For the donor star, solar composition ($X = 0.70$, $Y = 0.28$, and $Z = 0.02$) is adopted. The effective Roche-lobe radius of the donor star is given by Eggleton (1983)

$$\frac{R_{\rm L}}{a} = \frac{0.49q^{2/3}}{0.6q^{2/3} + \ln(1 + q^{1/3})}, \quad (1)$$

where a is the orbital separation, and $q = M_{\rm d}/M_{\rm NS}$ is the mass ratio of the binary.

2.2. Mass Transfer

When the donor star evolves to fill its Roche lobe, the material is transferred to the NS at a rate of $\dot{M}_{\rm tr}$ (<0) via Roche-lobe overflow. MESAbinary offers two choices for the mass-transfer schemes (Paxton et al. 2015). Here we use the default binary control parameters, which utilize the Ritter scheme (Ritter 1988). During the mass exchange, the accretion process onto the NS is limited to the Eddington accretion rate

$$\dot{M}_{\rm Edd} = 1.8 \times 10^{-8}\left(\frac{M_{\rm NS}}{1.4M_\odot}\right)\left(\frac{0.2}{\eta}\right)\left(\frac{1.7}{1+X}\right)M_\odot\ {\rm yr}^{-1}, \quad (2)$$

where $\eta = GM_{\rm NS}/(R_{\rm NS}c^2)$ is the energy conversion efficiency (G is the gravitational constant, $R_{\rm NS}$ is the NS radius, and c is the speed of light in vacuo). In this work, a constant NS radius of $R_{\rm NS} = 10^6$ cm is adopted, and X is the hydrogen abundance in the accreting material. Similar to Podsiadlowski et al. (2002), the accretion efficiency of the NS is assumed to be 0.5; thus, the fraction of transferred mass that is lost from the vicinity of the NS is

$$\beta = \begin{cases} 0.5, & -\dot{M}_{\rm tr} \leqslant 2\dot{M}_{\rm Edd} \\ \dfrac{\dot{M}_{\rm tr} + \dot{M}_{\rm Edd}}{\dot{M}_{\rm tr}}, & -\dot{M}_{\rm tr} \geqslant 2\dot{M}_{\rm Edd}. \end{cases} \quad (3)$$

The accretion rate of the NS can then be written as

$$\dot{M}_{\rm NS} = -(1-\beta)\dot{M}_{\rm tr}. \quad (4)$$

In addition, we also consider irradiation-driven winds. In a compact binary, the stellar wind from the donor star induced by the X-ray radiation cannot be ignored during the accretion of the NS (Ruderman et al. 1989; Tavani & London 1993). van Haaften et al. (2013) found that irradiation of the donor star plays a vital role in forming UCXBs with an orbital period longer than 40 minutes. A fraction of the X-ray luminosity ($L_{\rm X} = \eta\dot{M}_{\rm NS}c^2$) that the donor star receives is assumed to drive a wind from the surface of the donor star and converted into the kinetic energy of the wind (with a velocity given by the escape speed from the donor's surface). Hence, the stellar wind-loss rate satisfies the relation

$$L_{\rm X}\frac{\pi R_{\rm d}^2}{4\pi a^2}f = -\frac{GM_{\rm d}\dot{M}_{\rm wind}}{R_{\rm d}}, \quad (5)$$

where $R_{\rm d}$ is the radius of the donor star, f is the wind-driving efficiency. The mass-loss rate of the donor star $\dot{M}_{\rm d} = \dot{M}_{\rm tr} + \dot{M}_{\rm wind}$.

2.3. Orbital Angular-momentum Loss Mechanisms

The loss of orbital angular momentum plays a vital role during the evolution of binary systems. In this work, the rate of orbital-angular-momentum loss of IMXBs consists of three terms

$$\dot{J} = \dot{J}_{\rm GR} + \dot{J}_{\rm ML} + \dot{J}_{\rm MB}. \quad (6)$$

In Equation (6), the first term $\dot{J}_{\rm GR}$ is produced by gravitational-wave radiation, given by (Landau & Lifshitz 1971)

$$\dot{J}_{\rm GR} = -\frac{32G^{7/2}}{5c^5}\frac{M_{\rm NS}^2M_{\rm d}^2(M_{\rm NS}+M_{\rm d})^{1/2}}{a^{7/2}}. \quad (7)$$

The second term in Equation (6) takes into account the orbital angular-momentum loss due to the systemic mass loss. It includes the mass loss from the irradiation-driven wind of the donor star and the mass outflow from the accreting NS. The former is thought to carry away the specific orbital angular momentum of the donor star. The latter should form an isotropic wind in the vicinity of the NS and is then ejected with the specific orbital angular momentum of the NS. Thus the angular-momentum loss rate becomes

$$\dot{J}_{\rm ML} = \frac{2\pi a^2}{(M_{\rm NS}+M_{\rm d})^2P_{\rm orb}}(M_{\rm NS}^2\dot{M}_{\rm wind} + \beta M_{\rm d}^2\dot{M}_{\rm tr}), \quad (8)$$

where $P_{\rm orb}$ is the orbital period of the binary.

The third term in Equation (6) specifies the angular-momentum loss rate caused by magnetic braking, which plays a key role leading to the formation of UCXBs in our model. We have already accounted for the direct influence of the irradiation-driven winds on the orbital evolution in $\dot{J}_{\rm ML}$. However, its indirect effect is much more important if the

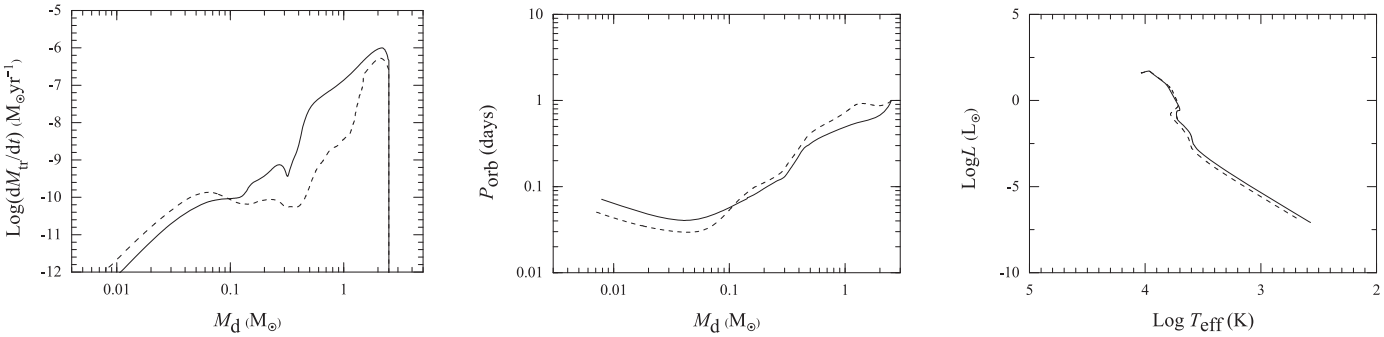

Figure 1. Mass-transfer rate (left panel) and orbital period (middle panel) as a function of the donor-star mass, HR diagram (right panel) of the donor star when the initial donor-star mass is 2.5 $M_\odot$ and the initial orbital period $P_{\rm orb,i} = 1.0$ day. The wind-driving efficiency $f = 10^{-3}$. The solid, and dashed curves represent the anomalous magnetic braking model with $B_{\rm s} = 1000$ G, and 100 G, respectively.

magnetic field is strong. It is generally thought that the stellar wind always couples to the stellar magnetic field up to the magnetospheric radius ($r_{\rm m}$) beyond which the magnetic field can no longer force the stellar wind to co-rotate. Because the wind material is tied to the magnetic field lines up to $r_{\rm m}$, its specific angular momentum is considerable larger than the specific angular momentum of the binary system (Verbunt & Zwaan 1981). Assuming that the irradiation-driven winds are expelled at the magnetospheric radius, the loss rate of angular-momentum loss produced by magnetic braking can be written as (Justham et al. 2006)

$$\dot{J}_{\rm MB} = \dot{M}_{\rm wind} r_{\rm m}^2 \frac{2\pi}{P_{\rm orb}} = -B_{\rm s} R_{\rm d}^{13/4} \sqrt{-\dot{M}_{\rm wind}}\, (GM_{\rm d})^{-1/4} \frac{2\pi}{P_{\rm orb}}, \quad (9)$$

where $B_{\rm s}$ is the surface magnetic field of the donor star.[3] Meanwhile, the donor star in a close binary should be tidally locked, which would continuously spin up (or spin down) the donor star until its spin is synchronized with the orbital motion (Patterson 1984). This implies that the angular momentum carried away in the magnetic wind is ultimately drawn from the orbital angular momentum of the binary, making magnetic braking an important orbital angular-momentum loss mechanism. From Equations (5) and (9), and combining $L_{\rm X} = \eta \dot{M}_{\rm NS} c^2$ and *Kepler*'s third law, the orbital angular-momentum loss rate due to magnetic braking can be found to be

$$\dot{J}_{\rm MB} = -\frac{B_{\rm s} c}{2} \sqrt{\frac{f\eta \dot{M}_{\rm NS} (M_{\rm NS} + M_{\rm d})}{a^5}} \left(\frac{R_{\rm d}^{19}}{G M_{\rm d}^3}\right)^{1/4}. \quad (10)$$

If the donor stars lose their radiative core, magnetic braking is assumed to cease (Rappaport et al. 1983; Spruit & Ritter 1983).

3. RESULTS

3.1. Wind-driving Efficiency $f = 10^{-3}$

Because $\dot{J}_{\rm mb} \propto B_{\rm s} f^{1/2}$, there is a degeneracy between $B_{\rm s}$ and f in Equation (10), and we can keep one fixed while we vary the other. Similar to Justham et al. (2006), in this subsection, we take a relatively large wind-driving efficiency $f = 10^{-3}$. To investigate the influence of the surface magnetic field on the evolution, we first compare in Figure 1 the evolutionary results for magnetic fields of 100 G and of 1000 G, respectively, for an IMXB with a donor star of 2.5 $M_\odot$ and an initial period of one day. As shown in this figure, a strong magnetic field can result in a very efficient angular-momentum loss rate and rapid mass transfer in most evolutionary stages, as expected from Equation (10). Interestingly, the system with the weaker magnetic field has a lower minimum period (see also the discussion in Section 4). For simplicity, we always take a 1000 G surface magnetic field in this work and examine the influence of the wind-driving efficiency f on the formation of UCXBs.

To understand the evolutionary history of UCXBs originating from this anomalous magnetic-braking model with irradiation, we plot the evolution of IMXBs with two initial donor-star masses and different initial orbital periods in the $P_{\rm orb}$–$M_{\rm d}$ plane (see also Figure 2). In order to evolve toward ultra-short orbital periods, the initial orbital period of the IMXBs should be near the so-called bifurcation period of 1.25 and 1.5 days, depending on the initial donor-star masses. The bifurcation period is defined as the longest initial orbital period that forms UCXBs within a Hubble time (van der Sluys et al. 2005a, 2005b); it strongly depends on the magnetic-braking efficiency and mass loss from the binary systems (Pylyser & Savonije 1988, 1989; Ergma et al. 1998; Podsiadlowski et al. 2002; Ma & Li 2009a). The minimum periods are very sensitive to the initial periods: as shown in Figure 2, higher initial periods tend to lead to lower minimum periods. In Table 1, we present some of the relevant evolutionary quantities of IMXBs with their respective bifurcation periods for different initial donor-star masses. Table 1 indicates that, for a long time during the donor stars' evolution, H in the center is almost exhausted, in agreement with the results given by Nelson et al. (1986) and Fedorova & Ergma (1989). High He abundances in the core result in a more compact donor star and correspondingly shorter orbital periods (Tutukov et al. 1987; Lin et al. 2011). Compared to the previous models, the anomalous magnetic braking increases the bifurcation period because of the more efficient angular momentum loss.

Figure 3 illustrates the evolutionary sequence for an IMXB with a 3 $M_\odot$ donor star and an initial orbital period of 1.5 days. After 0.29 Gyr of nuclear evolution, the donor star starts to fill its Roche lobe when hydrogen in the center is almost exhausted (at this point, $X_{\rm c} = 0.0436$ and $Y_{\rm c} = 0.937$, i.e., the donor star

[3] Equation (9) is based on a simple analytical model for the physical process of magnetic braking. We cannot use the model given by Verbunt & Zwaan (1981), which is an empirical model to reproduce observed spin rates of low-mass stars, which is not directly applicative to Ap/Bp stars with their relatively strong magnetic fields.

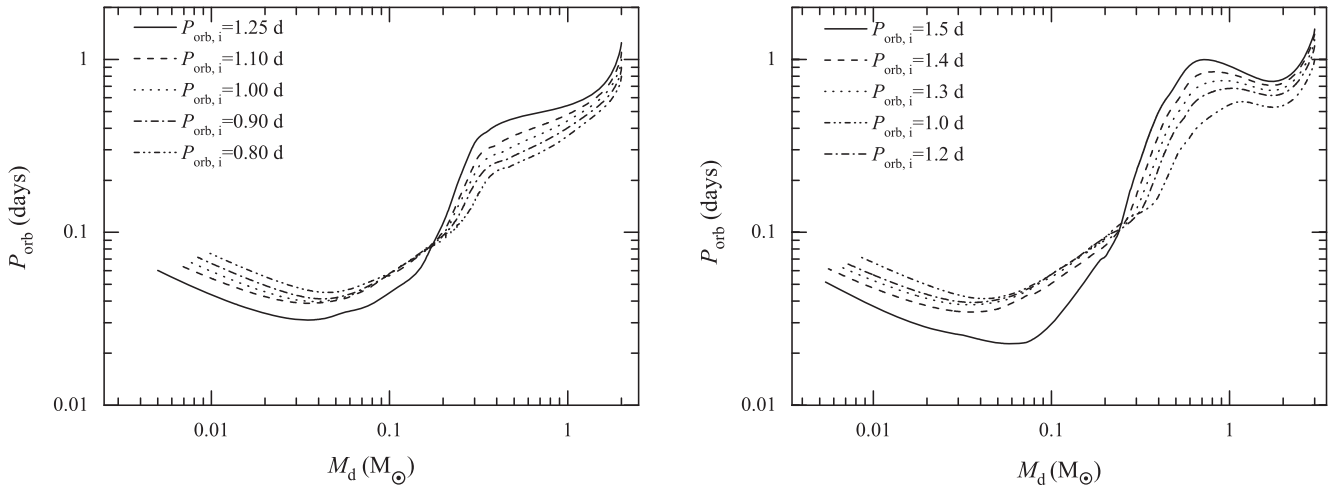

Figure 2. Evolutionary tracks of binary systems with different initial donor-star masses and initial orbital periods in the $P_{\rm orb}$–$M_{\rm d}$ diagram. The wind-driving efficiency $f = 10^{-3}$. The left and right panels denote the evolution of IMXBs with donor stars of 2.0 and 3.0 $M_\odot$, respectively.

Table 1
Selected Evolutionary Properties for IMXBs with Different Initial Donor-star Masses

$M_{\rm d,i}$ ($M_\odot$)	$P_{\rm bif}$ (days)	$P_{\rm rlov}$ (days)	$X_{\rm c,rlov}$	$Y_{\rm c,rlov}$	$P_{\rm min}$ (min)	$M_{\rm d,min}$ ($M_\odot$)	log $\dot{M}_{\rm d,min}$ ($M_\odot$ yr^{-1})
1.6	1.03	1.01	0.05	0.93	43	0.035	−10.2
1.8	1.15	1.09	0.08	0.90	49	0.036	−10.3
2.0	1.27	1.21	0.06	0.92	44	0.036	−10.2
2.2	1.33	1.31	0.04	0.94	40	0.034	−10.2
2.4	1.36	1.31	0.06	0.92	44	0.036	−10.2
2.6	1.42	1.41	0.05	0.93	40	0.034	−10.2
2.8	1.44	1.43	0.06	0.92	38	0.035	−10.2
3.0	1.50	1.49	0.04	0.94	32	0.061	−9.7
3.2	1.46	1.44	0.09	0.90	47	0.036	−10.3
3.4	1.40	1.39	0.12	0.86	52	0.035	−10.5

Note. We list the initial donor-star mass, the bifurcation period, the orbital period at the beginning of Roche-lobe overflow, the central H and He abundances at the beginning of Roche-lobe overflow, the minimum period, the donor-star mass, and the mass-transfer rate at the minimum period. The wind-driving efficiency $f = 10^{-3}$.

is near the end of the main sequence). Because the material is transferred from the more massive donor star to the less massive NS, mass transfer first occurs on the thermal timescale of the donor at a rate of 10^{-7}–$10^{-6}\,M_\odot$ yr^{-1}. Once the mass ratio is less than one, the mass-transfer rate changes to a sub-Eddington rate. From $t \sim 0.3$ to 1 Gyr, the mass-transfer rate is in the range of 10^{-10}–$10^{-9}\,M_\odot$ yr^{-1} and then sharply decreases to a very low value. At $P_{\rm orb} = 1.7$ hr, the angular-momentum loss rate due to gravitational radiation begins to exceed that due to magnetic braking. The orbital period of the binary continues to decrease and reaches a period minimum of 32 minutes when $t = 1.15$ Gyr. At some point, magnetic braking turns off because the radiative core vanishes (at this point, the remaining donor star has a low-mass He core). At $t = 0.97$ Gyr, the IMXB enters a phase where the period enters the UCXB regime (with decreasing period evolution) and stays in this regime until $t = 3.8$ Gyr, when its orbital period exceeds 1 hr again. Therefore, our simulation shows that the active UCXB lifetime in the period-decreasing and period-increasing phases are ∼0.2 Gyr and ∼2.6 Gyr, respectively.

To explore the initial parameter space for the progenitors of UCXBs formed by anomalous magnetic braking, we have calculated the evolution of a large number of IMXBs in the $P_{\rm orb,i}$–$M_{\rm d,i}$ plane, which was divided into 10×13 discrete grids. The IMXBs that can evolve into an ultra-short orbital period of less than 60 minutes in 13 Gyr are indicated as filled circles in Figure 4. The right boundary at 3.4 $M_\odot$ indicates the maximum mass beyond which mass transfer from the donor star would be dynamically unstable. Such dynamical mass transfer would most likely give rise to the spiral-in of the NS inside the donor star and the subsequent merger of the system (Podsiadlowski et al. 2002). The solid curve shows the bifurcation period of IMXBs for different donor-star masses. IMXBs with longer orbital periods evolve into binary millisecond pulsars with a He WD and a long orbital period. It is impossible to evolve into UCXBs in the Hubble time for the IMXBs below the bottom boundary. The exact location in this parameter space depends, however, on the surface magnetic field and the wind driving efficiency of the donor star.

Table 2 lists the orbital periods and average mass-transfer rates of 10 persistent sources and five transient sources. The mean mass-transfer rates can be derived from the time-averaged X-ray luminosity when the mass and the radius of the NS are assumed to be 1.4 $M_\odot$ and 11.5 km, respectively (Cartwright et al. 2013; Heinke et al. 2013). To compare our models with observations, we plot the evolution of an IMXB with an initial donor-star mass of 3 $M_\odot$ and an initial orbital period of 1.5 days in Figure 5. The evolutionary results of the standard magnetic braking ($\gamma = 4$) given by Verbunt & Zwaan (1981) and Rappaport et al. (1983) are also shown in this figure (here we assume that the standard magnetic braking model works when the donor star develops a convective envelope). It is clear that our simulated result is consistent with the observed data for three persistent sources and four transient sources. Moreover, the mass-transfer rates of the five transient sources are clearly lower than the critical mass-transfer rate for the disk-instability model (van Paradijs 1996; Dubus et al. 1999):

$$\dot{M}_{\rm cr} \simeq 3.2 \times 10^{-9}\left(\frac{M_{\rm NS}}{1.4M_\odot}\right)^{0.5}\left(\frac{M_{\rm d}}{1M_\odot}\right)^{-0.2}\left(\frac{P_{\rm orb}}{1\ {\rm day}}\right)^{1.4} M_\odot\ {\rm yr}^{-1}. \quad (11)$$

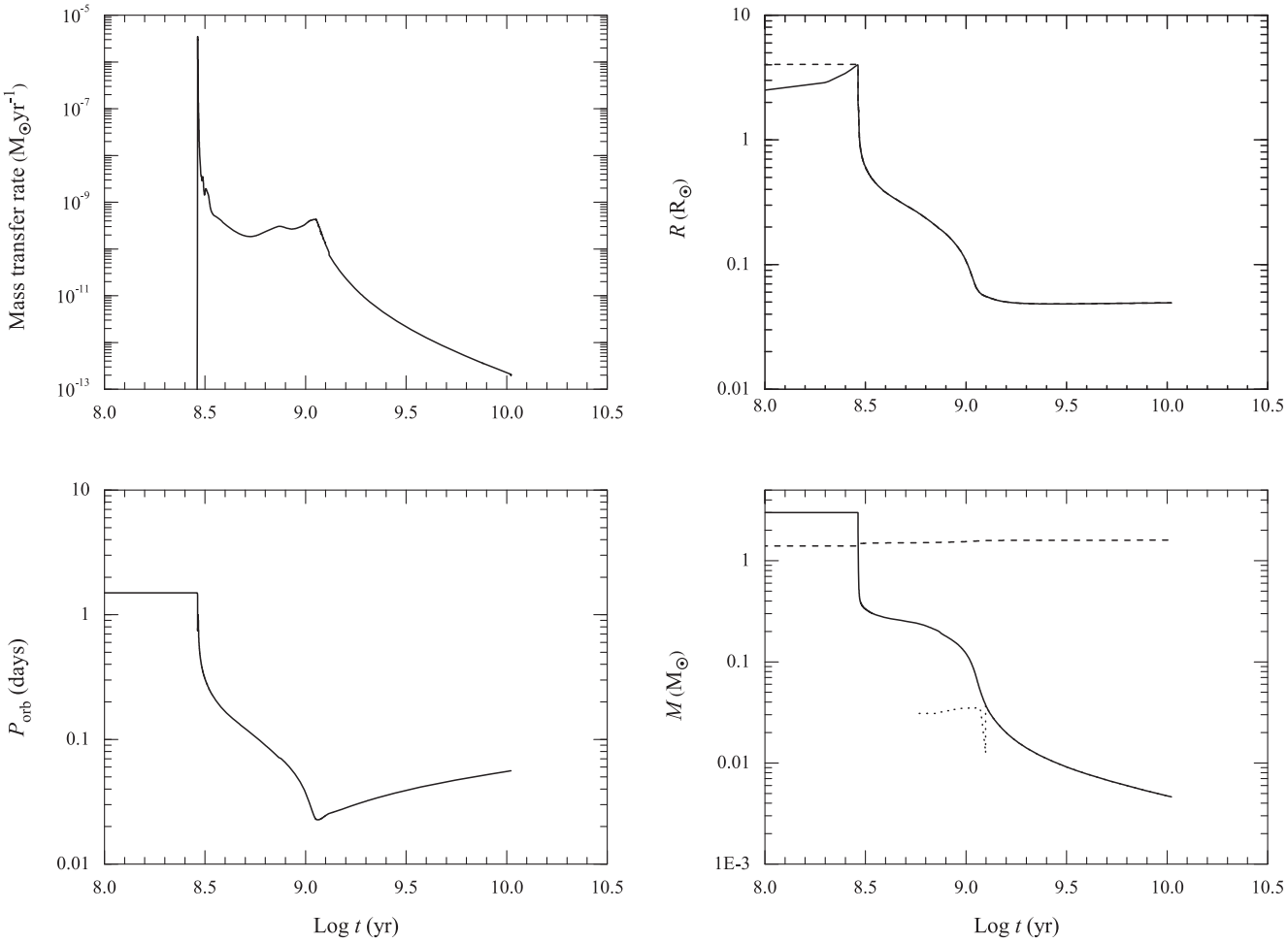

Figure 3. Evolution of the main binary parameters as a function of the donor-star age from the zero-age main sequence for an IMXB with a donor-star mass of 3 $M_\odot$ and an initial period of 1.5 days. The wind-driving efficiency $f = 10^{-3}$. Top left panel: mass-transfer rate. Bottom left panel: orbital period. Top right panel: radius (solid curve) and Roche-lobe radius (dashed curve) of the donor star. Bottom right panel: mass of the donor star (solid curve), NS (dashed curve), and the core (dotted curve).

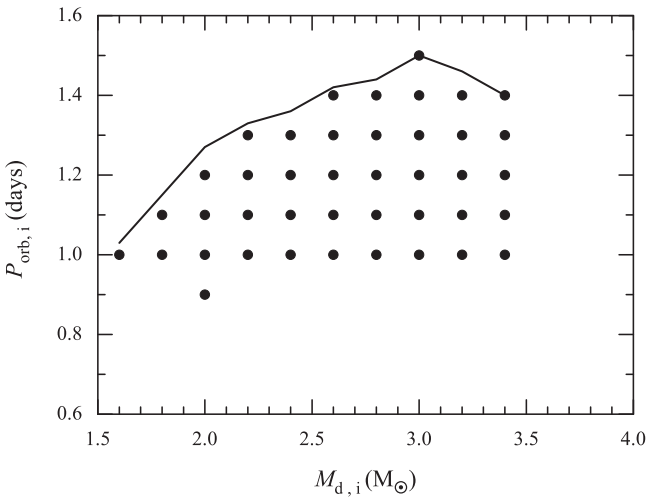

Figure 4. Parameter space distribution of the progenitor systems of UCXBs formed by the anomalous magnetic braking evolutionary channel (within 13 Gyr, with $f = 10^{-3}$) in the initial orbital vs. initial donor-star mass diagram. The solid curve represents the bifurcation period of IMXBs for different donor-star masses.

Below this critical rate, the accretion disk would experience thermal/viscous instabilities, where the accreting NSs are observed as transient X-ray sources with short-lived outbursts separated by long phases of quiescence. According to our simulations, five of the transient sources should be in the period-increasing phase, which, in principle, might be testable by timing observation in the future.

3.2. Wind-driving Efficiency $f = 10^{-5}$

To form UCXBs with an ultra-short period ($\lesssim$20 minutes), we calculated the evolution of some IMXBs adopting a relatively small wind-driving efficiency $f = 10^{-5}$. According to Equation (10), the angular-momentum loss rate in this case is approximately the same as the one with $B_s = 100$ G and $f = 10^{-3}$. However, the evolution of the donor stars is quite dramatically different. In Figure 6, we plot the evolutionary tracks of IMXB with a donor-star mass of 3 $M_\odot$ and an initial orbital period of 1.08 days. The donor star begins to fill its Roche lobe on the main sequence (when $X_c = 0.247$, and $Y_c = 0.737$). Due to the low irradiation wind loss, at $t = 9$ Gyr,

Table 2
Average Mass-transfer Rates and Orbital Periods of Some UCXBs

Source	$P_{\rm orb}$ (minutes)	$\langle \dot{M}_{\rm tr} \rangle$ ($M_\odot$ yr^{-1})	References
Persistent Sources			
4U 1728-34	10.8	$2.6 \pm 1.6 \times 10^{-9}$	1
4U 1820-303	11	$1.2 \pm 0.8 \times 10^{-8}$	2, 3
4U 0513-40	17	$1.2 \pm 0.6 \times 10^{-9}$	2, 4
2S 0918-549	17.4	$2.6 \pm 1.5 \times 10^{-10}$	5, 6
4U 1543-624	18.2	$1.3^{+1.8}_{-1.2} \times 10^{-9}$	7
4U 1850-087	20.6	$2.8 \pm 1.4 \times 10^{-10}$	2, 8
M15 X-2	22.6	$3.8 \pm 1.9 \times 10^{-10}$	2, 9
4U 1627-67	42	$8^{+14}_{-6} \times 10^{-10}$	10
4U 1916-053	50	$6.3 \pm 3.7 \times 10^{-10}$	11, 12, 13
4U 0614+091	51	$3.9 \pm 2.3 \times 10^{-10}$	14, 15
Transient Sources			
XTE J1807-294	40.1	$<1.9^{+2.6}_{-1.6} \times 10^{-11}$	16, 17
XTE J1751-305	42	$5.1^{+2.6}_{-2.9} \times 10^{-12}$	18, 19
XTE J0929-314	43.6	$<9.7^{+25}_{-7.7} \times 10^{-11}$	16, 20
Swift J1756.9-2508	54.7	$1.9^{+2.5}_{-1.7} \times 10^{-11}$	21
NGC 6440 X-2	57.3	$1.3 \pm 0.7 \times 10^{-12}$	2, 22

References. (1) Galloway et al. (2010), (2) Harris (2010), (3) Stella et al. (1987), (4) Zurek et al. (2009), (5) in't Zand et al. (2005), (6) Zhong & Wang (2011), (7) Wang & Chakrabarty (2004), (8) Homer et al. (1996), (9) Dieball et al. (2005), (10) Chakrabarty (1998), (11) Yoshida (1993), (12) Walter et al. (1982), (13) Iaria et al. (2015), (14) Brandt et al. (1992), (15) Shahbaz et al. (2008), (16) Galloway (2006), (17) Markwardt et al. (2003), (18) Papitto et al. (2008), (19) Markwardt et al. (2002), (20) Galloway et al. (2002), (21) Krimm et al. (2007), (22) Altamirano et al. (2010).

the donor star develops a He core of 0.105 $M_\odot$ (the maximum mass of the He core is ~0.03 $M_\odot$ when $f = 10^{-3}$). After the He core overflows its Roche lobe, it triggers a phase of relatively high mass transfer at a rate of 10^{-9}–$10^{-8}\,M_\odot$ yr^{-1}. When $t = 9.45$ Gyr, the binary reaches an ultra-short period of 11 minutes; at this point, the mass-transfer rate attains a maximum of $2.1 \times 10^{-8}\,M_\odot$ yr^{-1}. Subsequently, the UCXB begins to widen its orbit. The timescale in the period-increasing and period-decreasing stages are ~0.1 and ~2 Gyr, respectively.

The evolutionary sequences using the standard magnetic braking model with $f = 0$ is also shown in Figure 6. The calculation shows that the standard magnetic braking formalism has a much higher efficiency than anomalous magnetic braking in extracting angular momentum, resulting in a high mass-transfer rate at an earlier stage. In this case, the UCXB reaches its minimum period of 16 minutes at an age of 2.39 Gyr, preceding the anomalous magnetic braking by 7 Gyr. Therefore, the standard magnetic braking may overestimate the angular-momentum loss rate. This problem had already been noted in observations of rapidly rotating stars with a spin period of less than two to five days in young open clusters (Queloz et al. 1998; Andronov et al. 2003), in which the timescale of angular-momentum loss appears to be approximately two orders of magnitude longer than the value predicted in the standard magnetic braking model. Some observations of coronal and chromospheric activity imply that the resulting magnetic braking attains a maximum at an orbital period of less than three days (Vilhu 1982; Vilhu & Rucinski 1983). Figure 7 presents the comparison of the angular-momentum loss rate of the three cases including the strong ($f = 10^{-3}$) and weak ($f = 10^{-5}$) anomalous magnetic braking and the standard magnetic braking ($f = 0$). When the donor-star mass decreases to 0.8 $M_\odot$ and 0.4 $M_\odot$, the standard magnetic braking begins to exceed the weak anomalous magnetic braking and the strong one, respectively. For a donor star less than 0.5 $M_\odot$, the angular-momentum loss rate by the standard magnetic braking is one order of magnitude greater than that of the weak anomalous magnetic braking. To interpret the period gap of cataclysmic variables, Verbunt (1984) proposed that the donor stars needs to have a magnetic field of $\gtrsim$100 G and a wind of $10^{-10}\,M_\odot$ yr^{-1}, which is compatible with our result.

Figure 8 shows that the initial parameter space for UCXBs formed by weak magnetic braking is much smaller than that for strong magnetic braking (see also Figure 4). Except for initial donor stars in the range of 1.6–2.0 $M_\odot$, the most massive IMXBs all have the same bifurcation period of 1.08 days. Compared to the weak anomalous magnetic braking, standard magnetic braking has a relatively long bifurcation period (1.10–1.12 days for donor stars of 2.4–3.4 $M_\odot$) and a slightly smaller initial parameter space.

Figure 5 also presents the predicted relation between the orbital period and the mass-transfer rate for the anomalous magnetic braking with $f = 10^{-5}$, and the standard magnetic braking with $f = 0$. In the final stage, the magnetic braking ceases in all cases and gravitational radiation becomes the dominant driving mechanism; so the evolutionary tracks are similar in the three cases. It is clear that the anomalous magnetic braking scenario with a small wind-driving efficiency can fit four persistent sources and four transient sources. However, this case cannot produce the long-period UCXBs with a relatively high luminosity. The standard magnetic braking model can fit the observed data of three persistent sources with long periods and four transient sources, which is similar to the anomalous magnetic braking with $f = 10^{-3}$.

4. DISCUSSION

It is difficult to form UCXBs with an orbital period of less than 10 minutes in our scenario. In this section, we first analyze the factors influencing the minimum period. In principle, the orbital evolution of X-ray binaries depends on the angular-momentum loss and the mass-transfer process. The rate of change of the orbital period satisfies the relation

$$\frac{\dot{P}_{\rm orb}}{P_{\rm orb}} = 3\frac{\dot{J}}{J} - 3\frac{\dot{M}_{\rm d}}{M_{\rm d}}(1 - q\alpha) + \frac{\dot{M}_{\rm NS} + \dot{M}_{\rm d}}{M_{\rm NS} + M_{\rm d}}, \quad (12)$$

where $\alpha = -\dot{M}_{\rm NS}/\dot{M}_{\rm d}$ is the ratio between the accretion rate of the NS and the mass-loss rate of the donor star. For X-ray binaries with an orbital period of less than 2 hr, angular-momentum loss via gravitational radiation surpasses that due to magnetic braking (Nelson & Rappaport 2003). Then, ignoring the angular momentum carried away by mass loss, $\dot{J} = \dot{J}_{\rm GR}$. In Equation (12), $\dot{P}_{\rm orb} = 0$ yields the minimum period. Therefore, the minimum period can be written as

$$P_{\rm orb,min} = 0.066\frac{m_{\rm NS}^{3/8} m_{\rm d}^{3/4} (m_{\rm NS} + m_{\rm d})^{-1/8}}{(1 - q\alpha)^{3/8} |\dot{m}_{\rm d}|^{3/8}} \text{ minutes}, \quad (13)$$

where $m_{\rm NS}$ and $m_{\rm d}$ are $M_{\rm NS}$ and $M_{\rm d}$ in units of solar masses, and $\dot{m}_{\rm d}$ is $\dot{M}_{\rm d}$ in units of $M_\odot$ yr^{-1}.

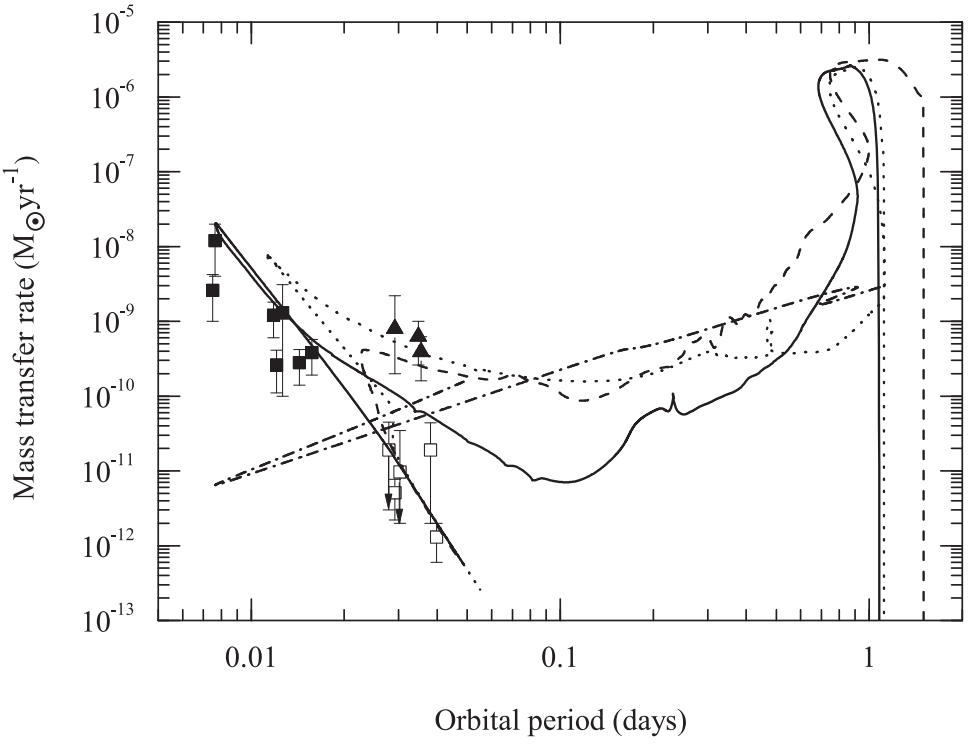

Figure 5. Evolution of IMXBs with an initial donor-star mass of 3 $M_\odot$ and a period just below the respective bifurcation period in the mass-transfer rate vs. orbital period diagram. The solid, dashed, and dotted curves represent the evolutionary tracks in the anomalous magnetic braking model with $f = 10^{-5}$ (with a bifurcation period of 1.08 days), $f = 10^{-3}$ (with a bifurcation period of 1.5 days), and the standard magnetic braking with $f = 0$ (with a bifurcation period of 1.12 days), respectively. The solid squares, solid triangles, and open squares denote seven persistent sources with a short orbital period, three persistent sources with a relatively long orbital period, and five transient sources, respectively. The dashed–dotted curve corresponds to the critical mass-transfer rate for the model track shown as a solid curve, below which systems should appear as transients.

In Figure 1, the high magnetic field leads to efficient angular-momentum loss and rapid mass transfer. For low magnetic fields with mass transfer occurring on a rather long timescale, the system develops a relatively tight orbit for the same donor-star mass. Because of the angular-momentum loss induced by the strong gravitational radiation, a relatively high mass-transfer rate is expected. When $f = 10^{-5}$, the massive He core that develops from the donor star leads to a more compact orbit, again resulting in a much higher mass-transfer rate.

In Figure 9, we show the relation between the minimum period and the mass-transfer rate for three different donor-star masses and a constant NS mass of 1.5 $M_\odot$. If the observed sources reach the minimum period during mass transfer, they should be located above the relevant curves at the present time (unless they experience a detached stage before the minimum period). According to this figure, the donor-star masses can be constrained to be near ~0.1, ~0.05, and ~0.01 $M_\odot$ for the three long-period persistent sources, seven short period persistent sources, and five transient sources, respectively. In Figure 5, our simulated results show that the relevant donor-star masses are in the range of 0.099–0.116, 0.0358–0.108, and 0.010–0.016 $M_\odot$, respectively. These inferred values are in approximate agreement with the calculated results.

Statistically, only a small fraction of A/B stars (about 5%) have anomalously strong magnetic fields and appear as Ap/Bp stars (Landstreet 1982; Shorlin et al. 2002). However, the populations formed via our evolutionary route should appear as UCXBs for a much longer time than in the circumbinary disk model (Ma & Li 2009b). The former spend 0.2 and 2.0 Gyr in the period-decreasing and period-increasing UXCB phases, while the lifetime of the latter is only 0.01 Gyr (there is no period-increasing stage in that model). Therefore, for the same birth rate of UCXBs, the number of observable systems formed by our scenario is approximately one order of magnitude larger than that in the circumbinary disk model. Compared to our evolutionary channel, the advantage of the circumbinary disk model is that it can drive LMXBs to an ultra-short period as short as six minutes; however, such a short-period UCXB has not yet been detected.

The irradiation wind-driving efficiency or magnetic field play an important role in influencing the formation of UCXBs such as the minimum period and the mass-transfer rate. A small $f = 10^{-5}$ or weak magnetic field ($B = 100$ G) can lead to minimum periods of 11 minutes, while a large $f = 10^{-3}$ may be applicable to the long-period persistent sources. Because the magnetic fields of the Ap/Bp stars are in the range of 100–10,000 G, the anomalous magnetic braking scenario provides a reasonable evolutionary channel toward various UCXBs.

5. CONCLUSIONS

It is generally thought that UCXBs with orbital periods <50 minutes cannot form by a modified magnetic braking mechanism (van der Sluys et al. 2005b) unless a circumbinary disk around L/IMXBs exists (Ma & Li 2009b). In this work, we propose an alternative evolutionary route toward forming UCXBs. Some IMXBs, which contain Ap/Bp stars with an anomalously strong magnetic field (100–10,000 G) may be able to produce UCXBs by anomalous magnetic braking with irradiation processes taken into account. To test the possibility of this new evolutionary channel for UCXBs, we have

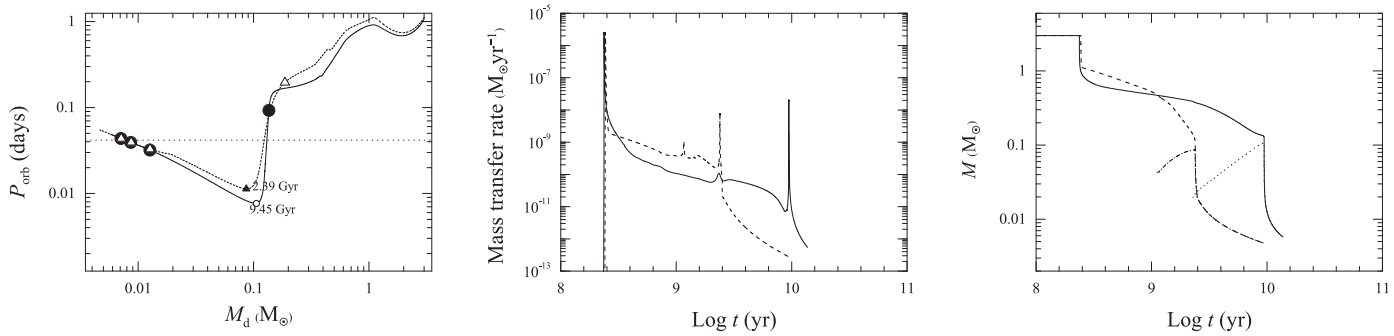

Figure 6. Evolutionary tracks of an IMXB with a donor-star mass of 3 $M_\odot$ for both the anomalous magnetic braking model with $f = 10^{-5}$ (with a bifurcation period of 1.08 days) and the standard magnetic braking model with $f = 0$ (with a bifurcation period of 1.12 days). The solid and dashed curves represent the evolutionary tracks of the anomalous magnetic braking and the standard magnetic braking, respectively. The horizontal dotted line in the left panel denotes the maximum period (1 hr) defining UCXBs. Left panel: orbital period as a function of donor mass; the solid circles along the solid curve indicate ages of 9, 10, 11, and 12 Gyr, respectively; the open triangles along the dashed curve represent ages of 2, 3, 4, and 5 Gyr, respectively. Middle panel: mass-transfer rate. Right panel: the mass of the donor star and the He core (the dotted and dashed–dotted curves represent the anomalous magnetic braking and the standard magnetic braking, respectively).

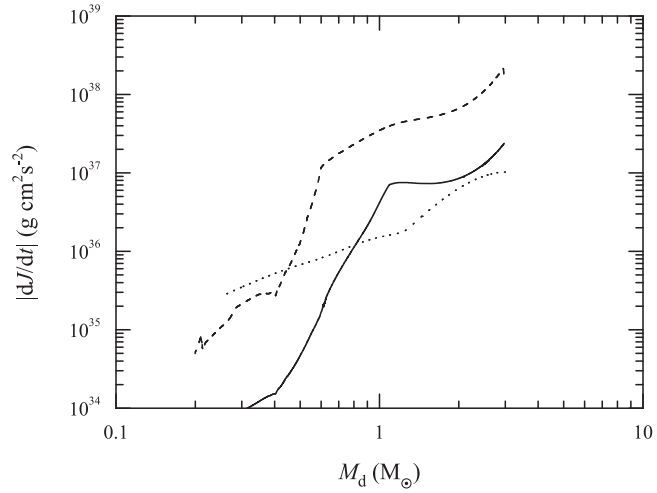

Figure 7. Angular-momentum loss rate as the function of the donor-star mass for an IMXB with a 3 $M_\odot$ donor star and an initial orbital period of 1.0 day. The solid, dashed, and dotted curves correspond to the anomalous magnetic braking with $f = 10^{-5}$ and $f = 10^{-3}$, and the standard magnetic braking with $f = 0$, respectively.

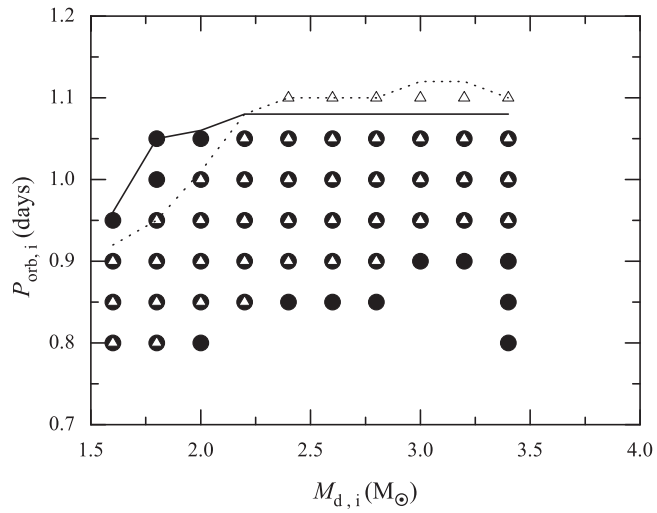

Figure 8. Similar to Figure 4, the solid circles and open triangles denote IMXBs evolved by the anomalous magnetic braking with $f = 10^{-5}$ and the standard magnetic braking with $f = 0$, respectively. The solid and dotted curves represent the bifurcation period of IMXBs evolved by the anomalous magnetic braking and the standard magnetic braking, respectively.

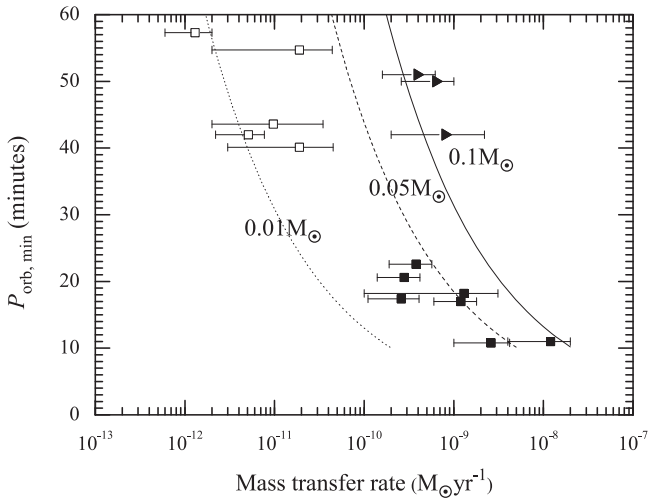

Figure 9. Minimum orbital period of UCXBs as a function of the mass-transfer rate if the orbital decay is only driven by gravitational radiation. The solid, dashed, and dotted curves correspond to donor-star masses of 0.1, 0.05, and 0.01 $M_\odot$, respectively. The other symbols are similar to those in Figure 5.

performed evolutionary calculations for a large number of IMXBs. Our main results are summarized as follows.

1. For donor stars with a 1000 G magnetic field, anomalous magnetic braking can evolve IMXBs into UCXBs with a minimum orbital period of 11 or 32 minutes (in our example calculations) when the irradiation wind-driving efficiency is $f = 10^{-5}$ and 10^{-3}, respectively. A smaller wind-driving efficiency or weaker magnetic field would give rise to a shorter orbital period.

2. Three long-period persistent UCXBs with relatively high mass-transfer rates of $\sim 10^{-9} M_\odot$ yr^{-1} can be produced by anomalous magnetic braking with a high irradiation wind-driving efficiency (10^{-3}) or a strong magnetic field. However, seven short-period persistent UCXBs favor a low wind-driving efficiency or weak magnetic field.

3. The evolutionary timescale of our simulated UCXBs in the period-increasing phase is generally much longer than that in the orbit-decaying phase. In the example presented in the paper, the evolutionary timescales in these two phases are $\sim$2 and 0.1 Gyr, respectively. Therefore, our scenario can produce relatively high birth rates despite the low fraction (5%) of Ap/Bp stars among intermediate-mass stars.

4. For intermediate-mass donor stars in the range of 1.6–3.4 $M_{\odot}$, IMXBs with orbital periods in the range of 0.9–1.5 days (for $f = 10^{-3}$; when $f = 10^{-5}$, the orbital period range changes to 0.8–1.08 days), the corresponding IMXBs can evolve into UCXBs.

5. Because H is almost exhausted in the center, IMXBs near the bifurcation period can reach the shortest orbital periods for a specific donor-star mass, similar to the conclusions drawn by Podsiadlowski et al. (2002) and van der Sluys et al. (2005a).

6. Our calculations indicate that the standard magnetic braking model may overestimate the angular-momentum loss rate for low-mass ($<0.8\,M_{\odot}$) donor stars. Though the angular-momentum loss rate by weak anomalous magnetic braking ($f = 10^{-5}$) is approximately one to two orders of magnitude lower than that in the standard magnetic braking model, it can still produce a much smaller minimum orbital period of 11 minutes, and has a much wider initial parameter space for forming UCXBs.

We are grateful to the anonymous referee for very helpful and useful suggestions. This work was partly supported by the National Science Foundation of China (under grant number 11573016), the Program for Innovative Research Team (in Science and Technology) in University of Henan Province, and the China Scholarship Council.

REFERENCES

Altamirano, D., Patruno, A., Markwardt, C. B., et al. 2010, ApJL, 712, L58
Andronov, N., Pinsonneault, M., & Sills, A. 2003, ApJ, 582, 358
Bailyn, C. D., & Grindlay, J. E. 1987, ApJL, 316, L25
Belczynski, K., & Taam, R. E. 2004, ApJ, 603, 690
Brandt, S., Castro-Tirado, A. J., Lund, N., et al. 1992, A&A, 262, L15
Cartwright, T. F., Engel, M. C., Heinke, C. O., et al. 2013, ApJ, 768, 183
Chakrabarty, D. 1998, ApJ, 492, 342
Davies, M. B., Benz, W., & Hills, J. G. 1992, ApJ, 401, 246
Davies, M. B., & Hansen, B. M. S. 1998, MNRAS, 301, 15
Deloye, C. J., & Bildsten, L. 2003, ApJ, 598, 1217
Dieball, A., Knigge, C., Zurek, D. R., et al. 2005, ApJL, 634, L105
Dubus, G., Lasota, J.-P., Hameury, J.-M., & Charles, P. 1999, MNRAS, 303, 139
Eggleton, P. P. 1983, ApJ, 268, 368
Ergma, E., Sarna, M. J., & Antipova, J. 1998, MNRAS, 300, 352
Fedorova, A. V., & Ergma, E. V. 1989, Ap&SS, 151, 125
Galloway, D. K. 2006, in AIP Conf. Proc. 840, The Transient Milky Way: A Perspective for MIRAX, ed. F. DAmico, J. Braga, & R. E. Rothschild (Melville, NY: AIP)
Galloway, D. K., Chakrabarty, D., Morgan, E. H., & Remillard, R. A. 2002, ApJL, 576, L137
Galloway, D. K., Yao, Y., Marshall, H., Misanovic, Z., & Weinberg, N. 2010, ApJ, 724, 417
Harris, W. E. 2010, arXiv:1012.3224
Heinke, C. O., Ivanova, N., Engel, M. C., et al. 2013, ApJ, 768, 184
Homer, L., Charles, P. A., Naylor, T., et al. 1996, MNRAS, 282, L37
Iaria, R., Di Salvo, T., Gambino, A. F., et al. 2015, A&A, 582, A32
Iben, I. J., Tutukov, A. V., & Yungelson, L. R. 1995, ApJS, 100, 233
in't Zand, J. J. M., Cornelisse, R., & Mendez, M. 2005, A&A, 440, 287
Ivanova, N., Chaichenets, S., Fregeau, J., et al. 2010, ApJ, 717, 948
Ivanova, N., Rasio, F. A., Lombardi, J. C., Jr., Dooley, K. L., & Proulx, Z. F. 2005, ApJL, 621, L109
Justham, S., Rappaport, S., & Podsiadlowski, P. 2006, MNRAS, 366, 1415
Krimm, H. A., Markwardt, C. B., Deloye, C. J., et al. 2007, ApJL, 668, L147
Landau, L. D., & Lifshitz, E. M. 1971, Classical Theory of Fields (Oxford: Pergamon Press)
Landstreet, J. D. 1982, ApJ, 258, 639
Lin, J., Rappaport, S., Podsiadlowski, P., et al. 2011, ApJ, 732, 70
Lombardi, J. C., Jr, Proulx, Z. F., Dooley, K. L., et al. 2006, ApJ, 640, 441
Ma, B., & Li, X.-D. 2009a, ApJ, 691, 1611
Ma, B., & Li, X.-D. 2009b, ApJ, 698, 1907
Markwardt, C. B., Juda, M., & Swank, J. H. 2003, ATel, 127, 1
Markwardt, C. B., Swank, J. H., Strohmayer, T. E., in't Zand, J. J. M., & Marshall, F. E. 2002, ApJL, 575, L21
Nelemans, G. 2009, CQGra, 26, 094030
Nelemans, G., Jonker, P. G., Marsh, T. R., & van der Klis, M. 2004, MNRAS, 348, L7
Nelemans, G., Jonker, P. G., & Steeghs, D. 2006, MNRAS, 370, 255
Nelson, L. A., & Rappaport, S. A. 2003, ApJ, 598, 431
Nelson, L. A., Rappaport, S. A., & Joss, P. C. 1986, ApJ, 304, 231
Papitto, A., Menna, M. T., Burderi, L., di Salvo, T., & Riggio, A. 2008, MNRAS, 383, 411
Patterson, J. 1984, ApJS, 54, 443
Paxton, B., Bildsten, L., Dotter, A., et al. 2011, ApJS, 192, 3
Paxton, B., Cantiello, M., Arras, P., et al. 2013, ApJS, 208, 4
Paxton, B., Marchant, P., Schwab, J., et al. 2015, ApJS, 220, 15
Podsiadlowski, P., Rappaport, S., & Pfahl, E. D. 2002, ApJ, 565, 1107
Pylyser, E. H. P., & Savonije, G. J. 1988, A&A, 191, 57
Pylyser, E. H. P., & Savonije, G. J. 1989, A&A, 208, 52
Queloz, D., Allain, S., Mermilliod, J.-C., Bouvier, J., & Mayor, M. 1998, A&A, 335, 183
Rappaport, S., Joss, P. C., & Webbink, R. F. 1982, ApJ, 254, 616
Rappaport, S., Verbunt, F., & Joss, P. C. 1983, ApJ, 275, 713
Rasio, F. A., Pfahl, E. D., & Rappaport, S. 2000, ApJL, 532, L47
Rasio, F. A., & Shapiro, S. L. 1991, ApJ, 377, 559
Ritter, H. 1988, A&A, 202, 93
Ruderman, M., Shaham, J., Tavani, M., & Eichler, D. 1989, ApJ, 343, 292
Savonije, G. J., de Kool, M., & van den Heuvel, E. P. J. 1986, A&A, 155, 51
Shahbaz, T., Watson, C. A., Zurita, C., Villaver, E., & Hernandez-Peralta, H. 2008, PASP, 120, 848
Shorlin, S. L. S., Wade, G. A., Donati, J.-F., et al. 2002, A&A, 392, 637
Sills, A., Pinsonneault, M. H., & Terndrup, D. M. 2000, ApJ, 534, 335
Spruit, H. C., & Ritter, H. 1983, A&A, 124, 267
Stella, L., Priedhorsky, W., & White, N. E. 1987, ApJL, 312, L17
Tavani, M., & London, R. A. 1993, ApJ, 410, 281
Tutukov, A. V., Fedorova, A. V., Ergma, E. V., & Yungelson, L. R. 1987, SvAL, 13, 328
Tutukov, A. V., & Yungelson, L. R. 1993, ARep, 37, 411
van der Sluys, M. V., Verbunt, F., & Pols, O. R. 2005a, A&A, 431, 647
van der Sluys, M. V., Verbunt, F., & Pols, O. R. 2005b, A&A, 440, 973
van Haaften, L. M., Nelemans, G., Voss, R., et al. 2013, A&A, 552, A69
van Haaften, L. M., Nelemans, G., Voss, R., Wood, M. A., & Kuijpers, J. 2012a, A&A, 537, A104
van Haaften, L. M., Voss, R., & Nelemans, G. 2012b, A&A, 543, A121
van Paradijs, J. 1996, ApJL, 464, L139
Verbunt, F. 1984, MNRAS, 209, 227
Verbunt, F. 1987, ApJL, 312, L23
Verbunt, F., & Zwaan, C. 1981, A&A, 100, L7
Vilhu, O. 1982, A&A, 109, 17
Vilhu, O., & Rucinski, S. M. 1983, A&A, 127, 5
Walter, F. M., Mason, K. O., Clarke, J. T., et al. 1982, ApJL, 253, L67
Wang, Z., & Chakrabarty, D. 2004, ApJL, 616, L139
Yoshida, K. 1993, PhD thesis, Tokyo Univ.
Yungelson, L. R., Nelemans, G., & van den Heuvel, E. P. J. 2002, A&A, 388, 546
Zhong, J., & Wang, Z. 2011, ApJ, 729, 8
Zurek, D. R., Knigge, C., Maccarone, T. J., Dieball, A., & Long, K. S. 2009, ApJ, 699, 1113